Colloid Polym Sci (2007) 285:423–430
DOI 10.1007/s00396-006-1584-6

ORIGINAL CONTRIBUTION

Reversible film formation from nano-sized PNIPAM particles below glass transition

Ş. Uğur · A. Elaissari · Ö. Yargi · Ö. Pekcan

Received: 20 April 2006 / Accepted: 15 September 2006 / Published online: 7 November 2006

Abstract Reversible film formation process from nano-sized Poly(*N*-isopropylacrylamide) (PNIPAM) microgel particles were studied during heating-cooling cycles at various rates. Photon transmission technique was used and transmitted photon intensity I_{tr} was monitored during heating–cooling cycles. The increase and decrease in I_{tr} during heating and cooling was explained with the void closure and void reconstruction processes, and the corresponding activation energies were measured. It was observed that PNIPAM microgels required less energy during reconstruction of voids than their closure.

Keywords Film formation · Nanoparticles · Poly (*N*-isopropylacrylamide) · Microgels

Introduction

In last decade, water-based polymer latexes have been gaining more attention in the coating and adhesives industries over conventional solvent-based systems, mainly due to restrictions imposed by environmental requirements. The mechanical properties of latex films are dependent on the molecular weight and its distribution [1, 2] and sensitivity to stabilizers [3] and surfactants [4]. In addition, the quality of these films, for a given molecular weight, depends on the annealing time and annealing temperature [5–8]. A temperature-sensitive poly(*N*-isopropylacrylamide) (PNIPAM) gel has been used in separation processes to extract water and low-molecular weight solutes from macromolecular solutions [9]. PNIPAM gels have also been used for enzyme, cell immobilization, and drug delivery [10]. It has been known that when a typical critical phase transition system undergoes a transition from one-phase state to two-phase coexisting state along the critical isochore (constant volume) path, the spinodal decomposition occurs.

In general, aqueous or non-aqueous dispersions of colloidal particles with glass transition temperature (T_g) above the drying temperature are named hard latex dispersion; however, aqueous dispersion of collodial particles with T_g below the drying temperature is called soft latex dispersions. The term "latex film" normally refers to a film formed from soft particles where the forces accompanying the evaporation of water are sufficient to compress and deform the particles into a transparent, void-free film [11, 12]. However, hard latex particles remain essentially discrete and undeformed during drying process. Film formation from these dispersion can occur in several stages. In both cases, the first stage corresponds to the wet initial state.

Evaporation of solvent leads to the second stage in which the particles form a close packed array, where, if the particles are soft, they are deformed to polyhedrons. Hard latex, however, stay undeform at this stage. Annealing of soft particles cause diffusion across particle–particle boundaries, which leads the film to a homogeneous

Ş. Uğur · Ö. Yargi
Department of Physics,
Istanbul Technical University, Maslak,
34469 Istanbul, Turkey

A. Elaissari
Macromolecular Systems and Human Immunovirology,
CNRS-bioMérieux,
UMR-2142 ENS de Lyon 46 allée d'Italie,
69364 Lyon Cedex, France

Ö. Pekcan (✉)
Department of Physics,
Işik University, Maslak,
34398 Istanbul, Turkey
e-mail: pekcan@isikun.edu.tr

continuous material. In annealing of hard latex systems, however, deformation of particles first leads to void closure [13, 14], and then after the voids disappear diffusion across particle–particle boundaries starts, i.e., the mechanical properties of hard latex films can be evolved by annealing, after all solvent has evaporated and all voids have disappeared.

PNIPAM dispersion was first synthesized using surfactant-free precipitation polymerization [15–20]. Similar to the behavior of the PNIPAM macrogel, the PNIPAM microgel particles swell in water at room temperature but shrink and undergo a reversible volume phase transition around 34 °C [21]. Because of its size, the microgel responds to environmental stimuli much faster than does the macrogel. The volume phase transition of the PNIPAM microgel has been studied and compared to that of bulk gels and linear polymers using light-scattering and small-angle neutron scattering techniques [22–25, 26]. Rheological properties of the PNIPAM dispersion have been investigated [13, 14].

The viscosity of the PNIPAM microgel dispersion can be changed by two orders of magnitude caused by temperature-induced swelling of the particles. The monodispersed PNIPAM microgel particles can form colloidal crystals and glasses in concentrated dispersions [27, 28]. The crystal structure of this material has been identified using small-angle neutron scattering techniques [29]. The crystal can be processed in its disordered state, and it can be reformed to its crystal state upon cooling [30]. On the other hand, ionized PNIPAM dispersion can be electrostatically stabilized, and colloidal crystal arrays are formed at low polymer content [31, 32]. Such an array has potential in sensor applications.

Transmission electron microscopy (TEM) has been used to examine the morphology of dried latex films [33]. These studies have shown that in some instances the particle boundaries disappeared over time, but in other cases the boundaries persisted for months. It was suggested that in former cases particle boundaries were healed by polymer diffusion across the junction. Small-angle neutron (SANS) has been used to examine deuterated particles in a protonated matrix [34].

More extensive studies have been performed using SANS by Sperling and coworkers [35] on compression-molded PS latex films. These works covered the interdiffusion process during film formation Alternatively, the process of interparticle polymer interdiffusion has been studied by direct nonradiative energy transfer (DET) using fluorescence decay measurements in conjunction with particles labeled with appropriate donor and acceptor chromophors [36–39]. This transient fluorescence technique has been used to examine latex film formation from PMMA and PBMA particles [37, 38].

These studies all indicate that in the particular systems examined, annealing the films above T_g leads to polymer polymer interdiffusion at the particle–particle junction as the particle interface heals. Stephen Mazur [40] has written an extensive review on coalescence of polymer particles, where he mainly discussed the neck growth mechanism and its several geometrical approximations before interdiffusion of polymer chains take place. More recently we performed various experiments with photon transmission method using UV–visible (UVV) spectrophotometer to study latex film formation from PMMA and PS latex particles where void closure and interdiffusion processes at the junction surfaces are studied [41, 42].

In this work, film formation from nano-sized poly (*N*-isopropylacrylamide) (PNIPAM) microgel particles, which were produced via precipitation polymerization process, was studied. Transmitted light intensities, I_{tr}, were measured by the photon transmission technique using the UV–visible spectrophotometer. The increase in I_{tr} intensity by increasing annealing temperature was explained with the void closure process. When the PNIPAM film was cooled back to room temperature, I_{tr} intensity decreased by a given hysteresis loop.

The behavior of I_{tr} was explained by the reversible film formation process. Void closure equation was derived and the activation energies of viscous flow during heating was measured. During cooling, reconstruction activation energies of microgel particles were measured and found to be much smaller than during viscous flow.

Experimental

PNIPAM preparation

Fluorescent poly *N*-isopropylyacrylamide microgel particles were synthesized via precipitation polymerization process. *N*-isopropylacrylamide (NIPAM) from Kodak was purified using a 60/40 (v/v) of hexane and toluene mixtures. Methylene bisacrylamide (MBA) from Aldrich was used as cross-linker monomer and was used when received. Fluorescent monomer 1-Pyrenylmethacrylate (PolyFluorTM 394) from Polysciences was also used.

The polymerization was performed using 1.2 g NIPAM, 0.059 g MBA, and 0.018 g potassium peroxodisulfate (KPS) as initiator. The recipe established by Menuier et al. [43, 44] was slightly modified by inducing well appropriate fluorescent (0.0054 g). All the reactants were first solubilized in water and introduced in the polymerization reactor. The polymerization was conducted (in 50 ml deionized water) under nitrogen atmosphere and at 70 °C. The polymerization reaction was carried out in 100-ml four-neck glass reactor equipped with a glass anchor-type

agitation (200 rpm), condenser, and nitrogen inlet. It reaction took place during 16 h.

The final conversion was gravimetrically determined and found to be 98.5%. The particles are fairly monodisperse, having all very similar mean diameters (close to 300 nm).

Film preparation and photon transmission

PNIPAM particles were dispersed in water in a test tube. Latex film was prepared from this dispersion by placing a certain number of drops on a glass plate (0.8×2.5 cm^2) and allowing the water to evaporate at room temperature. The annealing process of microgel particles was performed in UVV spectrophotometer in air below T_g (135 °C) of PNIPAM after the evaporation of water in 18, 9.4, 4.7, 3.0, and 2.3 °C/min heating rates from 10 to 100 °C. Transmitted photon intensity, I_{tr}, from the film samples was detected at 400 nm by UVV spectrophotometer (Jasco V-530). A glass plate was used as *a standard* for all UVV experiments. Errors in UVV measurements originate mostly from the surface inhomogeneities (voids and cracks) of film samples, which cause variation in I_{tr} intensities.

Noise-to-signal ratio in I_{tr} is quite low (1–2%) and can be neglected in error estimations. The temperature was maintained within the ±0.2 °C during annealing. Atomic force microscopy (AFM) images were obtained by SPM-9500-J3 Shimadzu scanning probe microscope.

Results and discussion

Transmitted photon intensities, I_{tr}, from PNIPAM films vs annealing temperature for 18.0, 9.4, 4.7, and 3.0 °C/min heating and cooling rates are presented in Fig. 1. Data in Fig. 1 indicate that films become more transparent, as they are annealed at higher temperatures. In other words, films scattered less light due to homogenization during film formation. The increase in I_{tr} may be interpreted by the mechanism of void closure process. Polymeric material in spherical particles that have increasing surface energy flow to intervoids (void closure) during annealing; as a result, the radius of interparticle voids decreases and film surface becomes more homogeneous, consequently transparency of film starts to increase.

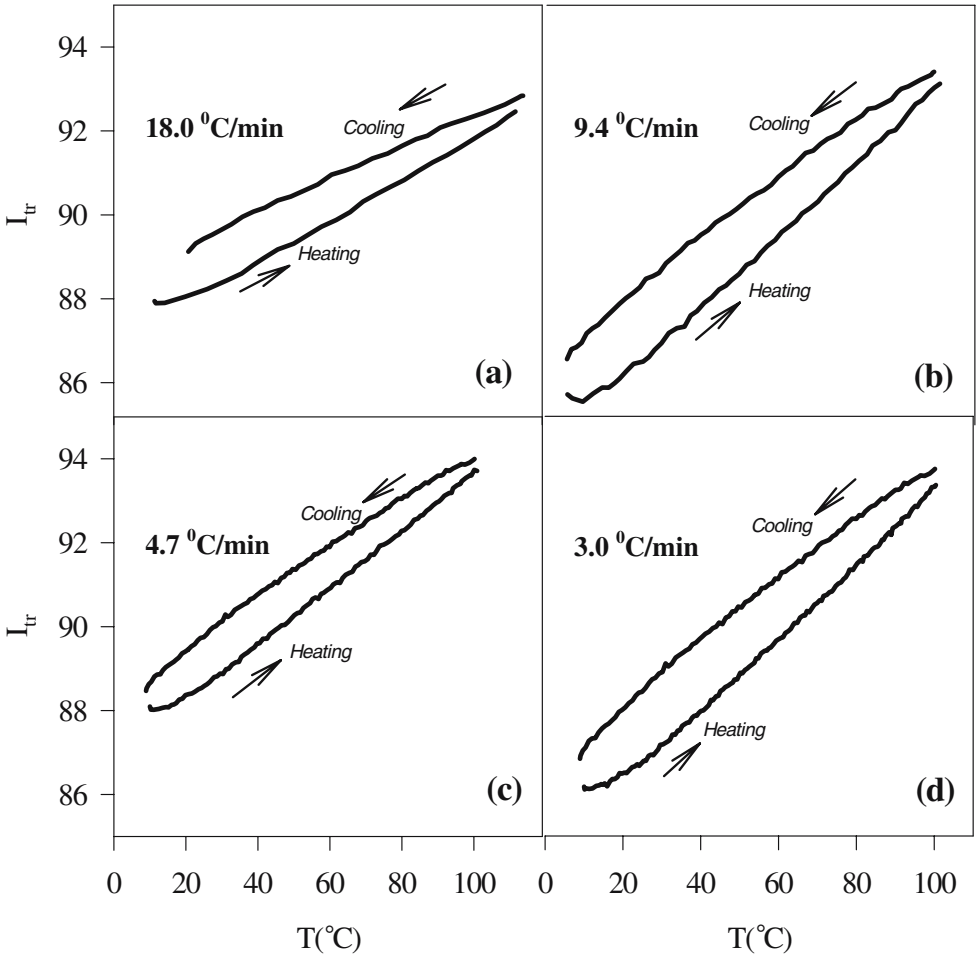

Fig. 1 Plot of transmitted photon intensities, I_{tr} from PNIPAM films against annealing temperature, *T*, during heating and cooling with the rates of **a** 18.0, **b** 9.4, **c** 4.7, and **d** 3.0 °C/min

On the other hand, when the PNIPAM film cooled back to room temperature, I_{tr} intensity decreased back to its initial value, indicating that the reversible film formation process took place. Polymeric material reversibly flow back and construct its original, spherical structure. Cartoon presentation of the above-mentioned picture is shown in Fig. 2. Voids disappeared after heating and an almost transparent film is formed, which can transmit more light. However, after cooling again film regains its original structure, which scatters light as high as its original form does.

These processes may be named as reconstruction process. It has to be mentioned in this paper that heating and cooling pathways are different, and present a hysteresis loop at all rates. Fig. 3a,b presents the AFM pictures of PNIPAM film before and after annealing. It is seen in Fig. 3b that no particle deformation can be detected after the annealing process is completed, which confirms the picture given in Fig. 2, by indicating that reversible film formation process takes place during a heating–cooling cycle.

Particle deformation and void closure

To quantify the behavior of I_{tr} during heating–cooling cycles, phenomenological void closure model is introduced. Particle deformation and void closure between particles can be induced by shearing stress, which is generated by surface tension of polymer, i.e., polymer–air interface. The void closure kinetics can determine the time for optical clarity and film formation [45]. An expression to relate the shrinkage of spherical void of radius r to the viscosity of surrounding medium η was derived and given by the following relation [13]. In Fig. 4 cartoon presentation of void closure process is given.

$$\frac{dr}{dt} = -\frac{\gamma}{2\eta}\left(\frac{1}{\rho(r)}\right), \tag{1}$$

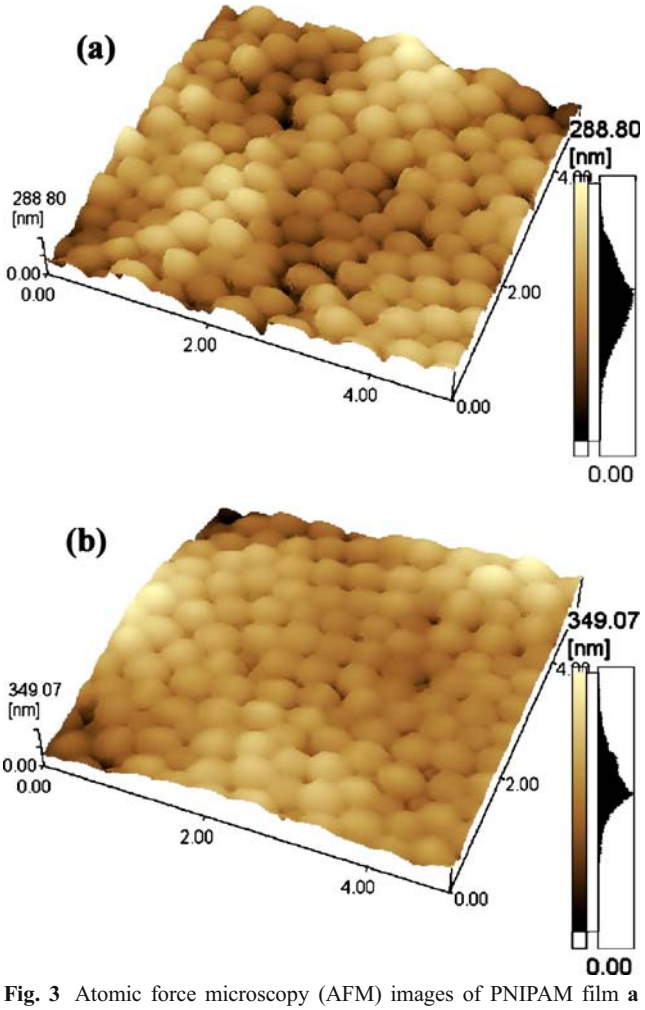

Fig. 3 Atomic force microscopy (AFM) images of PNIPAM film **a** before and **b** after annealing

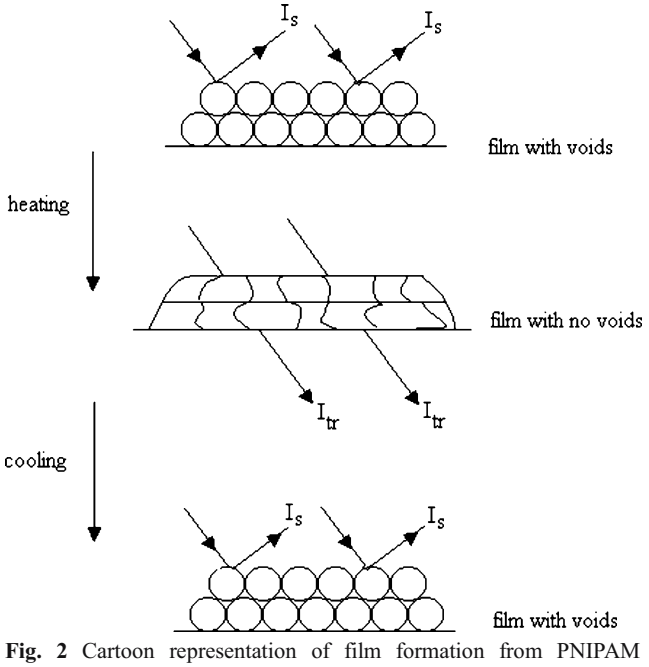

Fig. 2 Cartoon representation of film formation from PNIPAM microgels during heating and cooling processes

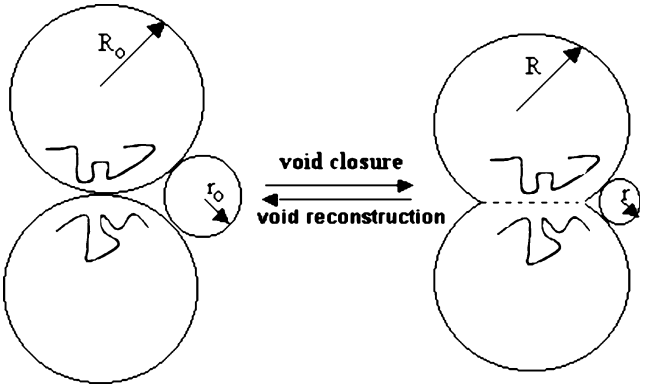

Fig. 4 Cartoon representation of void closure and reconstruction process. (R_0, r_0) and (R, r) are the initial and final particle and void radii, respectively

where γ is the surface energy, t is time, and $\rho(r)$ is the relative density.

It has to be noted that here surface energy causes a decrease in void size and the term $\rho(r)$ varies with the microstructural characteristics of the material, such as the number of voids, the initial particle size, and packing. Here $\rho(r)$ can be defined as a volume ratio of polymeric material to voids, whereas r goes to zero $\rho(r)$ increases; however, for large r values $\rho(r)$ it decreases.

Equation 1 is quite similar to one that was used to explain the time dependence of the minimum film formation temperature during latex film formation [14, 46]. If the viscosity is constant in time, integration of Eq. 1 gives the relation as

$$t = -\frac{2\eta}{\gamma}\int_{r_0}^{r}\rho(r)\mathrm{d}r, \tag{2}$$

where r_o is the initial void radius at time t=0.

The dependence of the viscosity of polymer melt on temperature is affected by the overcoming of the forces of macromolecular interaction, which enables the segments of polymer chain to jump over from one equilibration position to another. This process happens at temperatures at which free volume becomes large enough and is connected with the overcoming of the potential barrier. The height of this barrier can be characterized by free energy of activation, ΔG, during viscous flow. The Frenkel–Eyring [47] theory produces the following relation for the temperature dependence of viscosity,

$$\eta = \frac{N_o h}{V}\exp\left(\Delta G/kT\right) \tag{3}$$

where N_0 is Avogadro's number, h is Planck's constant, V is molar volume, and k is Boltzman constant. It is known that $\Delta G = \Delta H - T\Delta S$, then Eq. 3 can be written as

$$\eta = A\exp\left(\Delta H/kT\right), \tag{4}$$

where ΔH is the activation energy of viscous flow, i.e., the amount of heat that must be given to one mole of material for creating the act of a jump during viscous flow. ΔS is the entropy of activation of viscous flow. Here A presents a

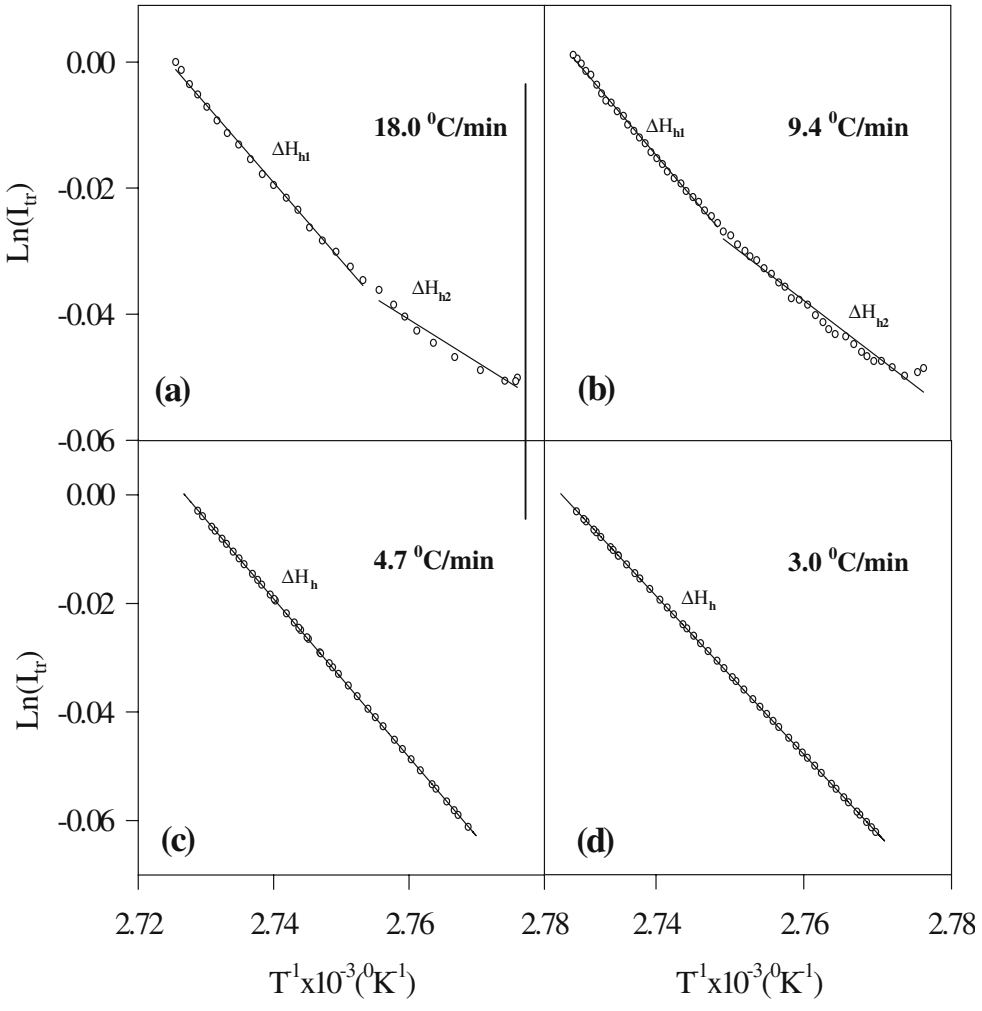

Fig. 5 Logarithmic plots of I_{tr} vs T^{-1} for PNIPAM films during heating process at **a** 18.0, **b** 9.4, **c** 4.7, and **d** 3.0 °C/min. The slope of the *straight lines* produce ΔH_{h1} and ΔH_{h2} void closure energies

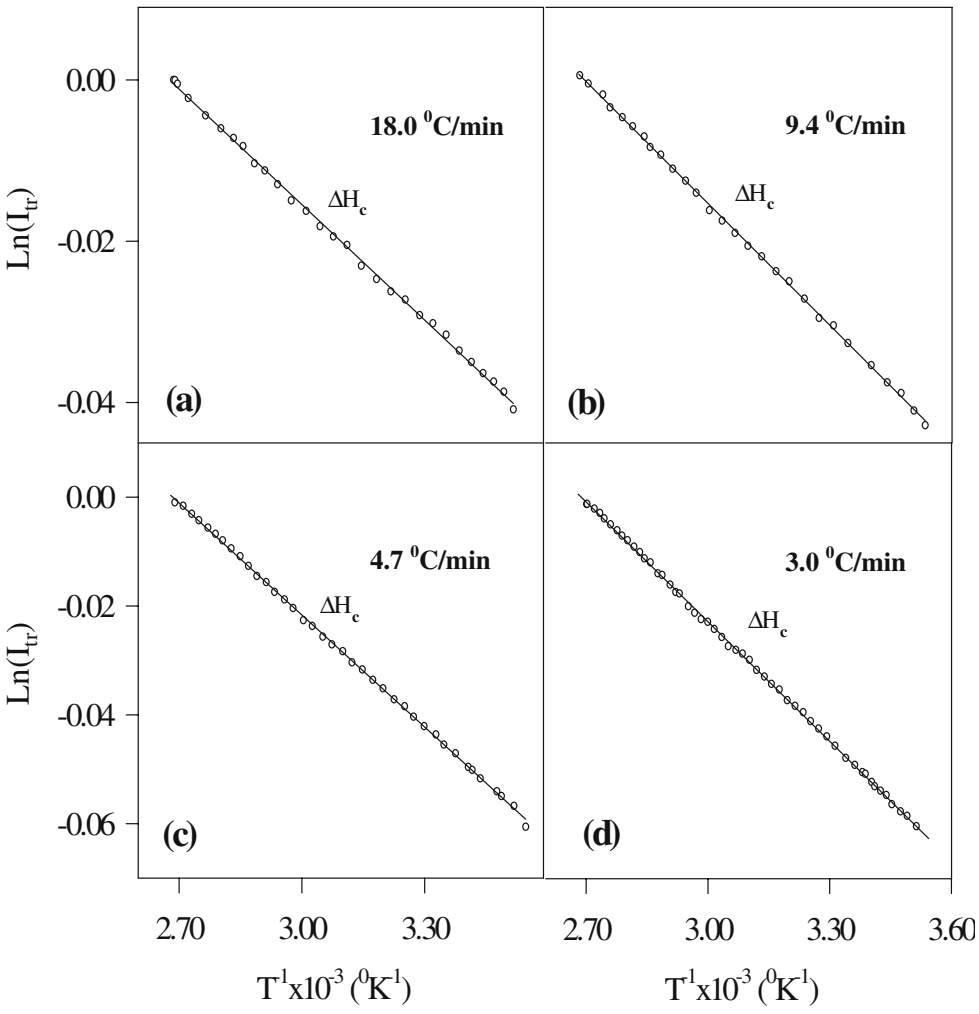

Fig. 6 Logarithmic plots of I_{tr} vs T^{-1} for PNIPAM films during cooling process at **a** 18.0, **b** 9.4, **c** 4.7, and **d** 3.0 °C/min. The slope of the *straight lines* produce ΔH_c void reconstruction energies

constant for the related parameters. Combining Eqs. 2 and 4, the following useful equation is obtained

$$t = -\frac{2A}{\gamma}\exp\left(\frac{\Delta H}{kT}\right)\int_{r_0}^{r}\rho(r)\mathrm{d}r. \tag{5}$$

Equation 5 can be employed by assuming that the interparticle voids are in equal size and number of voids that stay constant during film formation (i.e., $\rho(r)\infty r^{-3}$), then integration of Eq. 5 gives the relation

$$t = \frac{2AC}{\gamma}\exp\left(\frac{\Delta H}{kT}\right)\left(\frac{1}{r^2}-\frac{1}{r_0^2}\right), \tag{6}$$

where C is a constant related to relative density $\rho(r)$. It is well established that decrease in void size causes an increase in mean free path of a photon, which then results

Table 1 ΔH values of heating and cooling rates

Rates	Values				
Heating and cooling rates (°C/min)	18	9.4	4.7	3.0	2.3
ΔH_{h1}(kJ/mol)	0.21	0.24	–	–	–
ΔH_{h2}(kJ/mol)	0.11	0.16	–	–	–
ΔH_h(kJ/mol)	–	–	4.04	4.04	4.04
ΔH_c (kJ/mol)	0.14	0.16	0.19	0.20	0.20

Void closure (ΔH_h) and void reconstruction (ΔH_c) activation energies produced from Figs. 5 and 6, respectively

in an increase in I_{tr} [41]. Then the assumption can be made that I_{tr} is inversely proportional to void radius r, and Eq. 6 can be written as

$$t = \frac{2AC}{\gamma} \exp\left(\frac{\Delta H}{kT}\right) I_{tr}^2, \tag{7}$$

Here r_0^{-2} is omitted from the relation, as it is very small compared to r^{-2} values after void closure processes start. Equation 7 can be solved for I_{tr} to interpret the results in Fig. 1 as

$$I_{tr}(T) = S(t) \exp\left(-\frac{\Delta H}{3kT}\right), \tag{8}$$

where $S(t) = \left(\gamma t/2AC\right)^{1/2}$. For a given time, the logarithmic form of Eq. 8 can be written as follows:

$$\ln I_{tr}(T) = \ln S(t) - \frac{\Delta H}{3kT}. \tag{9}$$

In I_{tr} vs T^{-1} plots of the data in Fig. 1 are presented in Figs. 5 and 6 for a 18.0, b: 9.4, c 4.7, and d 3.0 °C/min time rates during heating and cooling processes, respectively. All the plots in Figs. 5 and 6 present a set of straight lines where void closure and void reconstruction processes take place, respectively. ΔH values in Eq. 9 were obtained from the slopes of straight lines in Figs. 5 and 6 and are listed in Table 1 for all heating–cooling cycles.

Here ΔH_h and ΔH_c values represent void closure and void reconstruction activation energies during the heating and cooling processes, respectively. The averaged ΔH_h value was found to be 4.0 kJ/mol at low heating rates. However, for high heating rates, two different activation energies in two different regions were observed. These results indicate that a void closure process can be accomplished in two stages at higher heating rates with much lower energy than the void closure at lower heating rates.

On the other hand, during cooling, activation energies ΔH_c were found to be much smaller than ΔH_h at low heating rates, which may predict that back flow needs lower energy during reconstruction of voids than void closure at these rates. In other words, reconstruction of voids during cooling is much easier than void closure process, and as a result requires much less energy at low rates. However, at high rates cooling activation energies ΔH_c were found to be very close to heating activation energies, ΔH_{h1} and ΔH_{h2}. Cooling activation energies were almost found to be independent of rates, which means polymer relaxation in bulk is unimportant for this particular system during cooling. On the other hand, heating activation energies were found to be strongly correlated to rates during heating.

In general, the activation energy of viscous flow, i.e., the dependence of viscosity on temperature, is determined by the structure of polymer chain. In other words, the type of branches and the presence of polar groups in the chain determine the kinetic flexibility of polymer. For carbon chain polymers, ΔH are found to be 20.9 to 29.26 kJ/mole (polyethylene). ΔH reaches the value of 62.7 kJ/mole for poly(iso butylene). For polystrene whose side groups are phenyl rings, ΔH rises to 117 kJ/mole. ΔH is much higher for poly(vinyl chloride) (146 kJ/mole) and poly(vinyl acetate) (251 kJ/mole) polymers [47].

Here, in our system ΔH values were found to be much smaller than the above-mentioned group of polymers. Most probably, PNIPAM microgels can easily be deformed in this temperature region due to its small sizes.

In conclusion, this work has presented a study on reversible film formation from nano-sized PNIPAM particles at high and low rates during heating-and-cooling cycles. It was shown that voids in PNIPAM film can disappear after annealing is completed; however, these voids can be created by cooling the system back to room temperature. This phenomenon itself is quite interesting, and an example for a stimuli-responsive system.

In this paper, it has been shown that a void closure process is strongly dependent on the heating rates; however, during reconstruction of voids, activation energies are found to be independent of rates. In other words, PNIPAM film responds to the temperature variation at different rates during void closure; on the other hand, void reconstruction process is not quite sensitive to the rates during cooling.

References

1. Mohammadi N, Klein A, Sperling LH (1993) Macromolecules 26:1019
2. Sambasivan M, Sperling LH, Klein A (1995) Macromolecules 28:152
3. Pekcan Ö, Arda E, Kesenci K, Pişkin E (1998) J App Polym Sci 68:1257
4. Sambasivan M, Klein A, Sperling LH (1995) J App Polym Sci 58 (2):357
5. Wang Y, Winnik MA (1996) J Phys Chem 97:2507
6. Canpolat M, Pekcan Ö (1995) Polymer 36:4433
7. Canpolat M, Pekcan Ö (1995) Polymer 36:2025
8. Pekcan Ö, Canpolat M (1996) J App Polym Sci 59:1699
9. Hirotsu S (1988) J Chem Phys 88:427
10. Hoffman AS, Afrassiabi A, Dong LC (1986) J Control Release 4:213
11. Eckersly ST, Rudin A (1990) J Coatings Technol 62(780):89
12. Joanicat M, Wong K, Maquet J, Chevalier Y, Pichot C, Graillat C, Linder P, Rios L, Cabane B (1990) Prog Coll Polym Sci 81:175
13. Sperry PR, Snyder BS, O'Dowd ML, Lesko PM (1994) Langmuir 10:2619
14. Mackenzie JK, Shutlewort R (1949) Proc Phys Soc 62:838
15. Pelton RH, Chibante P (1986) Colloids Surf 120:247
16. Chan K, Pelton RH, Zhang J (1999) Langmuir 15:4018
17. Zhang J, Pelton RH (1999) Langmuir 15:8032
18. Zhang J, Pelton RH, Deng Y (1995) Langmuir II:2301
19. Tam KC, Ragaram S, Pelton RH (1994) Langmuir 10:418
20. Pelton RH, Pelton HM, Morfesis A, Rowell RL (1989) Lanqmuir 5:816

21. Hirotsu S, Hirokawa Y, Tanaka T (1987) J Chem Phys 87:1392
22. Wu C (1998) Polymer 39:4609
23. Wu C, Zhou SQ (1996) Macromolecules 29:1584
24. Wu C (1997) J Macromol Sci Phys 36:345
25. Wang XH, Qiu XP, Wu C (1988) Macromolecules 31:2972
26. Lee LT, Cabane B (1997) Macromolecules 30:6559
27. Kiminta OD, Luckham PF, Lenon S (1995) Polymer 36:4827
28. Snowden MJ, Choudhry BZ, Vincent B, Morris GE (1996) J Chem Soc Faraday Trans 92:5013
29. Hellweg T, Dewhurst CD, Brucker E, Kratz K, Eimer W (2000) Colloid Polym Sci 278:972
30. Debord JD, Lyon LA (2000) J Phys Chem 104:6327
31. Weissmann JM, Sunkara HB, Tse AS, Asher SA (1996) Science 274:959
32. Holtz JH, Asher SA (1997) Nature 389:829
33. Distler D, Kanig G (1978) Colloid Polym Sci 256:1052
34. Hahn K, Ley G, Schuller H, Oberthur R (1988) Colloid Polym Sci 66:631
35. Kim KD, Sperling LH, Klein A (1993) Macromolecules 26:4624
36. Pekcan Ö, Winnik MA, Croucher MD (1990) Macromolecules 23:2673
37. Bozcar EM, Dionne BC, Fu Z, Kirk AB, Lesko PM, Koller AD (1993) Macromolecules 26:5772
38. Zhao CL, Wang Y, Hruska Z, Winnik MA (1990) Macromolecules 23:4082
39. Wang Y, Zhao CL, Winnik MA (1991) J Chem Phys 95:2143
40. Mazur S (1996) Coalescence of polymer particles. In: Maukis M, Rosenweig V (eds) Polymer powder technology. Wiley
41. Pekcan Ö, Arda E (1999) Colloids Surf A 153:537
42. Arda E, Bulmuş V, Pişkin E, Pekcan Ö (1999) J Coll Int Sci 213:160
43. Meunier F, Elaissari A, Pichot C (1995) Preparation and characterization of cationic poly(*N*-Isopropylacrylamide) copopolymer latexes. Pol Adv Tech 6:489
44. Meunier F, Elaissari A (2003) Poly(*N*-Isopropylacrylamide)-based particles: preparation and colloidal characterization. Surfactant Sci Ser 115:117–144
45. Keddie JL, Meredith P, Jones RAL, Ronald AM (1995) Proceedings of the American Chemical Society conference, vol. 73, p 144
46. Mc Kenna GB (1989) In: Booth C, Price C (eds) Comprehensive polymer science, vol. 2. Pergamon, Oxford
47. Tager A (1978) Physical chemistry of polymers. MIR, Moscow